Near-field Shaping by Leaky-Wave Metasurfaces: OAM and Bessel Beams Synthesis

M. Bodehou, C. Craeye, and I. Huynen

***Abstract*—We present and discuss the synthesis of Leaky-wave (LW) radiating metasurfaces for near-field applications. The metasurface sheet transition Impedance Boundary Condition (IBC) is computed after discretizing the relevant Electric Field Integral Equation (EFIE) with Fourier-Bessel basis functions. We have shown that the near-field of the MTS can be controlled with a very good accuracy, down to a height of about one wavelength from the surface. Several examples have been successfully designed, which cover Bessel beam radiators for focusing applications and multiple OAM beams. The designed MTSs are numerically validated with the Method of Moments (MoM).**

***Index Terms*—Near-field focusing, OAM beams, modulated metasurfaces, method of moments, bessel beams.**

I. Introduction

Modern imaging, sensing and communication systems require an accurate shaping of the near-field radiation. Possible applications concern the generation of Orbital Angular Momentum (OAM) beams [1]-[5], non-diffractive Bessel beams for near-field focusing [6]-[8] or Magnetic Resonance Imaging (MRI) systems [9]. Accurately shaping the near-field is still a big challenge nowadays and sometimes requires complex/expensive or specific systems, depending on the required near-field effect. On the other hand, metasurfaces emerge as a very promising technology due to their unique property of controlling waves at subwavelength level [10]. This calls for a proper synthesis of artificial surfaces, which present in frequency bands, unusual electromagnetic properties. Such structures have recently demonstrated their effectiveness for applications involving space waves transmission [11], surface-wave (SW) wavefront manipulation, and LW antennas [12]. Metasurfaces excited by SWs are of particular interest in space applications since the structure can be made extremely flat and low profile [13]. The aperture field synthesis of such surfaces is carried out after modulating an anisotropic impedance boundary condition (IBC). The IBC properly describes the fields at the MTS in the homogenization limit. The present paper is dealing with electric sheet IBC, which is defined as the ratio between the aperture electric field and the surface current. The IBC is synthesized in a circular domain and is excited by a centered SW launcher [14]. Such a tensorial IBC can be implemented by means of printed patches with small slots, as already demonstrated in several papers [13], [15]. As proven in [16] and [17], a sinusoidal or locally sinusoidal modulation of a capacitive-sheet IBC leads to the appearance of several harmonics of the fundamental SW. In antenna applications, one may design the IBC in order to radiate only one of such harmonics. However, in the case of near-field shaping, others harmonics can play an important role if they are very close to the visible region. Recently, a formalism based on the Electric Field Integral Equation (EFIE) has been proposed to design circular domain [18] (or possibly elliptical domain [19], [20]) MTS antennas. In this framework, the IBC modulation is no longer necessarily sinusoidal, but it is simply described in a Fourier-Bessel basis. The Fourier-Bessel functions form a complete set of orthogonal and entire-domain basis functions, which serve to describe the current distribution as well as the sheet IBC modulation. The sheet IBC is printed on top of a grounded substrate. Our interest in the present paper consists of proving that the EFIE formalism can be used to accurately control the near-field of the metasurface down to distances very close to the surface (about one wavelength). In particular, we focus our attention on the generation of non-diffractive Bessel beams, and OAM beams.

This paper is structured as follows. Section II summarizes the design methodology, section III presents some numerical results, and section IV draws some conclusions.

II. Metasurface design

We consider a circular domain sheet transition IBC $\underline{\underline{\mathbf{Z}}}_S(\boldsymbol{\rho})$ of the following form:

$$\begin{aligned} Z_S^{\rho\rho}(\rho,\phi) &= Z_0^{\rho\rho} + P^{\rho\rho}(\rho,\phi) \\ Z_S^{\rho\phi}(\rho,\phi) &= Z_S^{\phi\rho}(\rho,\phi) = P^{\rho\phi}(\rho,\phi) \\ Z_S^{\phi\phi}(\rho,\phi) &= Z_0^{\phi\phi} - P^{\rho\rho}(\rho,\phi) \end{aligned} \tag{1}$$

where $\underline{\underline{\mathbf{Z}}}_0 = diag(Z_0^{\rho\rho},\ Z_0^{\phi\phi})$ is the average impedance, ρ and ϕ are the cylindrical coordinates of a given point. Since we are dealing with TM excited SWs, $\underline{\underline{\mathbf{Z}}}_0$ is assumed to be purely capacitive. Such IBCs can be projected into the Fourier-Bessel basis as follows:

$$Z_S^{\rho\rho} \approx \sum_{n_S,m_S} [K_S^{\rho\rho}(m_S,n_S) + X_S^{\rho\rho}(m_S,n_S)]\ R_{m_S,n_S} \tag{2}$$

$$Z_S^{\rho\phi} \approx \sum_{n_S,m_S} X_S^{\rho\phi}(m_S,n_S)\ R_{m_S,n_S} \tag{3}$$

$$Z_S^{\phi\phi} \approx \sum_{n_S,m_S} [K_S^{\phi\phi}(m_S,n_S) - X_S^{\rho\rho}(m_S,n_S)]\ R_{m_S,n_S} \tag{4}$$

where $K_S^{\rho\rho}(m_S,n_S)$ and $K_S^{\phi\phi}(m_S,n_S)$ correspond respectively to the expansion coefficients of the average impedances $Z_0^{\rho\rho}$ and $Z_0^{\phi\phi}$. $X_S^{\rho\rho}$ and $X_S^{\rho\phi}$ are the unknown IBC reactance modulations discretized into FBBFs. Finally, R_{m_S,n_S} are the FBBFs defined over the whole circular domain of radius a as follows:

$$R_{m,n}\left(\frac{\rho}{a},\phi\right) = J_n\left(\lambda_n^m \frac{\rho}{a}\right) e^{-jn\phi} \tag{5}$$

978-1-7281-0563-5/19/$31.00 ©2019 IEEE

where λ_n^m is the m-th positive zero of $J_n(x)$ (the first kind Bessel function of order n). In the absence of modulation, namely considering only the average impedance $\underline{\underline{\mathbf{Z}}}_0$, a TM SW can be supported by the MTS. The wavenumber of such a wave is $k_{sw} = k_0\sqrt{1+(X_{op}/\eta_0)^2}$ where jX_{op} is the impenetrable surface impedance, and η_0 is the free-space impedance. X_{op} is obtained after adding to $\underline{\underline{\mathbf{Z}}}_0$ the contribution of the grounded substrate. For near-field applications, k_{sw} should be taken as far as possible from k_0 since the excited SW exhibits an exponential decay $e^{-\alpha z}$ from the surface, with $\alpha = \sqrt{k_{sw}^2 - k_0^2}$. In this way, the SW contribution can be neglected, even staying very close to the surface. This implies the choice of a high value of the opaque (impenetrable) impedance.

The IBC satisfies the following integral equation [21], [22]:

$$\hat{\mathbf{z}} \times \left[\iint_{S'} \underline{\underline{\mathbf{G}}}^{EJ}(\boldsymbol{\rho}, \boldsymbol{\rho}')\ \mathbf{J}(\boldsymbol{\rho}')\ dS' - \underline{\underline{\mathbf{Z}}}_S(\boldsymbol{\rho})\ \mathbf{J}(\boldsymbol{\rho}) \right] = -\hat{\mathbf{z}} \times \mathbf{E}_i \tag{6}$$

where $\underline{\underline{\mathbf{G}}}^{EJ}$ is the substrate Green's function, $\mathbf{E}_i$ is the MTS excitation, and $\mathbf{J}$ is the surface current distribution.

As proven in [18], expression (6) can be solved to derive, from the knowledge of the current $\mathbf{J}$ and that of the excitation $\mathbf{E}_i$, the needed tensorial IBC $\underline{\underline{\mathbf{Z}}}_S$. Moreover, the IBC can be constrained (in a least-squares sense) to be anti-Hermitian (property required in the absence of loss), which leads to the following operator:

$$\underline{\underline{\mathbf{X}}}_S = l.s.\left\{EFIE^{-1}(\mathbf{J})\right\} \tag{7}$$

The reader is referred to [18] for more details.

The objective of the present paper consists of synthesizing a given aperture electric field $\mathbf{E}(x,y)$. We assume that the maximum spectral component k_{max} of $\mathbf{E}(x,y)$ is lower than k_0, i.e $\tilde{\mathbf{E}}(k_x,k_y) = 0$ for $k_\rho > k_0$ with k_0 being the free-space wavenumber. The difference with the procedure described in [18], lies in the way the current $\mathbf{J}$ is found. Indeed, since the desired aperture field is known, one can directly project it into FBBFs and add the contribution of the SW, rather than starting from the radiation pattern as done in [18], [19].

III. Results

We present the design of Bessel and OAM beams. The antenna is excited at the center ($\rho = 0$) by a vertical point source, as in [18]-[22]. The operating frequency is 20 GHz. The substrate has a relative permittivity of $\epsilon_r = 3.66$ and a thickness $d = 1.52$ mm. The antenna radius is $a = 10\lambda$ and the average reactance is $X_0 = -383\ \Omega$.

A. Non diffractive bessel beams

This section discusses the synthesis of a propagating Bessel beam launcher. Such beams have already been designed in [23] with metasurfaces using a Geometrical Optics approximation. The desired radiated aperture field is [7]:

$$E_\phi = 0$$
$$E_\rho = j\frac{k_z}{k_\rho}J_1(k_\rho \rho)$$

where $k_\rho^2 + k_z^2 = k_0^2$, and k_0 is the free-space wavenumber. $J_n(x)$ is the first kind Bessel function of order n. As shown in [7], such a tangential aperture electric field is consistent with a z-directed electric field

$$E_z = J_0(k_\rho \rho)e^{-jk_z z} \tag{8}$$

This means that the electric field profile does not change/diffract with respect to z. However, one needs an infinite aperture size to generate (8). The truncation of the radiating aperture leads to the definition of a non-diffractive range along z [23]:

$$z_{max} = a\sqrt{\left(\frac{k_0}{k_\rho}\right)^2 - 1} \tag{9}$$

where a is the antenna radius. In this paper, we choose $k_\rho = 0.51k_0$, which leads to $z_{max} \approx 16.8\ \lambda$. Once the MTS IBC computed, the z-directed electric field is calculated as follows. First, the MoM algorithm presented in [22] is used to compute the surface current $\mathbf{J}$. Then the tangential aperture electric field is computed as $\tilde{\mathbf{E}} = \underline{\underline{\tilde{\mathbf{G}}}}^{EJ}\ \tilde{\mathbf{J}} + \tilde{\mathbf{E}}_i$, where $\underline{\underline{\tilde{\mathbf{G}}}}^{EJ}$ and $\tilde{\mathbf{E}}_i$ correspond respectively to the spectral Green's function of the substrate and the spectral electric field of the excitation on the MTS. In spectral domain, the z-component of the electric field is related to the x and y components through $\tilde{E}_x k_x + \tilde{E}_y k_y = -\tilde{E}_z k_z$. From there, one can compute the spatial field E_z through a simple Fourier transform:

$$E_z = -\frac{1}{4\pi^2}\iint \frac{e^{-j(k_x x + k_y y + k_z z)}}{k_z}(\tilde{E}_x k_x + \tilde{E}_y k_y)\ dk_x dk_y \tag{10}$$

Since the fields are TM polarized, ($\tilde{E}_x(k_x,k_y) = \tilde{E}_0(k_\rho)\cos\alpha,\ \tilde{E}_y(k_x,k_y) = \tilde{E}_0(k_\rho)\sin\alpha$), where k_ρ and α are the spectral variables in cylindrical coordinates. After inserting the latter expression in (10) and analytically integrating along α, the 2D integral (10) reduces to a 1D integral

$$E_z = -\frac{1}{2\pi}\int_0^\infty \frac{J_0(k_\rho \rho)}{k_z}e^{-jk_z z}\ \tilde{E}_0(k_\rho)\ k_\rho^2\ dk_\rho \tag{11}$$

Integral (11) can be evaluated over a contour in the complex plane to avoid the poles appearing at $k_z = 0$ and those from the substrate Green's function. Note that the integrand rapidly converges to zero for non-negligible heights z due to the presence of the exponential factor. Fig. 1 illustrates a map of E_z in the plane $\phi = 0^o$ corresponding to the desired bessel beam. Fig. 2 shows the designed IBC modulation. It can be seen that the $\rho\phi$ component of the IBC is almost zero, which is consistent with the purely TM nature of the Bessel Beam. Fig. 3(a) shows a map of E_z in the plane $\phi = 0^o$, generated by the designed MTS. One can observe the focusing effect over the whole non-diffractive region ($z \leq 16.8\lambda$). Fig. 3(b) compares cuts (corresponding to the axis ($z = 1\lambda,\ \phi = 0^o$) and ($z = 16\lambda,\ \phi = 0^o$)) with the one obtained from equation (8), which assumes an infinite aperture size. One can observe a good agreement on the main lobe and first side lobes at $z = 1\lambda$. Differences are mainly due to the finite size of the structure and the direct space wave radiation of the feed. The latter issue could be solved to a large extent by designing a specific SW launcher. Closely to the non-diffractive range,

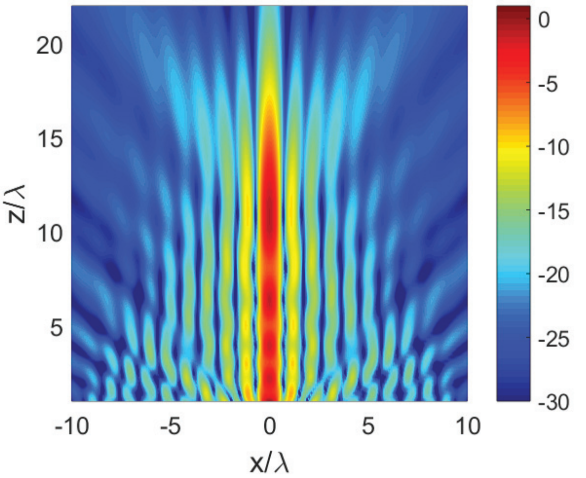

Fig. 1: Normalized electric field z-component (in dB) of the desired bessel beam.

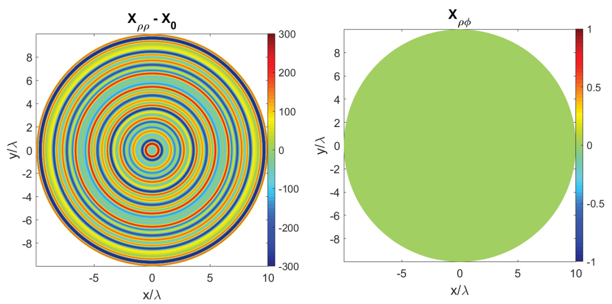

(a) (b)

Fig. 2: IBC Modulation for the synthesized Bessel beam radiating MTS (a) $X_{\rho\rho} - X_0$ (b) $X_{\rho\phi}$.

namely at $z = 16\lambda$, the differences are more important, specially on the side lobes, due to the diffraction effects.

B. Multi-OAM beams

The second example concerns a MTS antenna radiating two circularly polarized OAM beams. Multiplexing with OAM beams is essentially limited to near-field links [3]. The desired radiated aperture field is given as

$$E_x = J_1\left(\lambda_1^1 \frac{\rho}{a}\right) e^{-j\phi} + 10\ J_1\left(\lambda_1^{10} \frac{\rho}{a}\right) e^{-j\phi}$$
$$E_y = jE_x$$

where λ_n^m is the m-th positive zero of the the first kind Bessel function of order n. Those beams correspond to the Fourier-Bessel Basis functions as defined in (5) and are therefore orthogonal on the disk. In [24], the transmittance between antennas radiating such OAM beams have been rigorously analyzed and a closed form expression of the transmittance has been proposed. Fig. 4 shows the derived modulation required to obtain the multi-OAM beams. Fig. 5(a), (b) illustrate the obtained radiation pattern in the (u, v) plane and Fig. 5(c) compares a cut in the plane $\phi = 0^o$ with that of an ideal antenna of the same radius, radiating the same beam. This ideal antenna radiation pattern has been computed after discretizing the desired field with Fourier-Bessel basis functions defined over the whole circular domain. One can observe an excellent agreement between the designed MTS radiation pattern and the desired one.

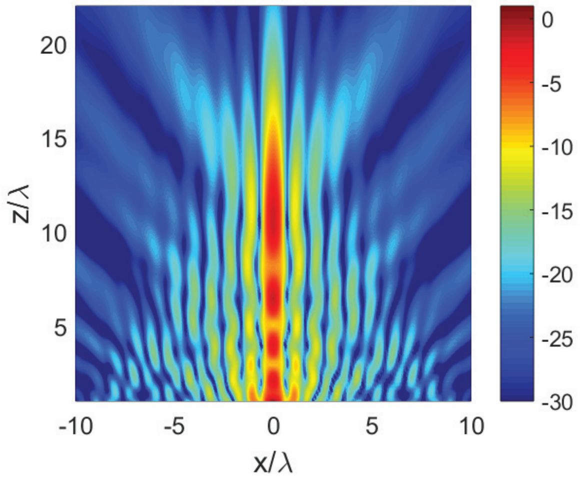

(a)

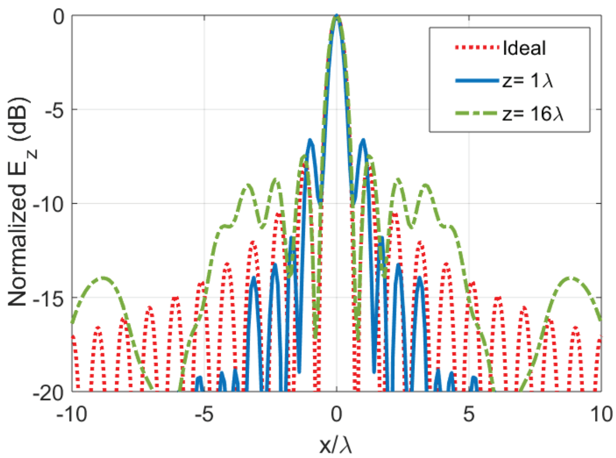

(b)

Fig. 3: Normalized electric field z-component (in dB) of the designed MTS Bessel beam radiator (a) Map in the plane $\phi = 0^o$ (b) Comparison of a cut in the axis $(z = 1\lambda,\ \phi = 0^o)$ and $(z = 16\lambda,\ \phi = 0^o)$, with the fields (8).

IV. Conclusion

Near-field shaping with LW modulated MTSs has been discussed through the synthesis of Bessel and multiple OAM beams. The obtained results demonstrate the capabilities of modulated MTSs for near-field applications down to distances of about one wavelength from the surface. The effectiveness of the method appears despite the fact the radiation originates from a surface-wave.

Acknowledgments

This research has been supported by a FRIA grant from the Belgium FNRS fund.

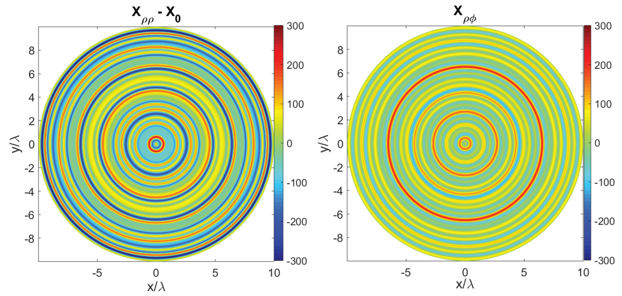

(a) (b)

Fig. 4: IBC Modulation for the synthesized multi-OAM beams radiating MTS (a) $X_{\rho\rho} - X_0$ (b) $X_{\rho\phi}$.

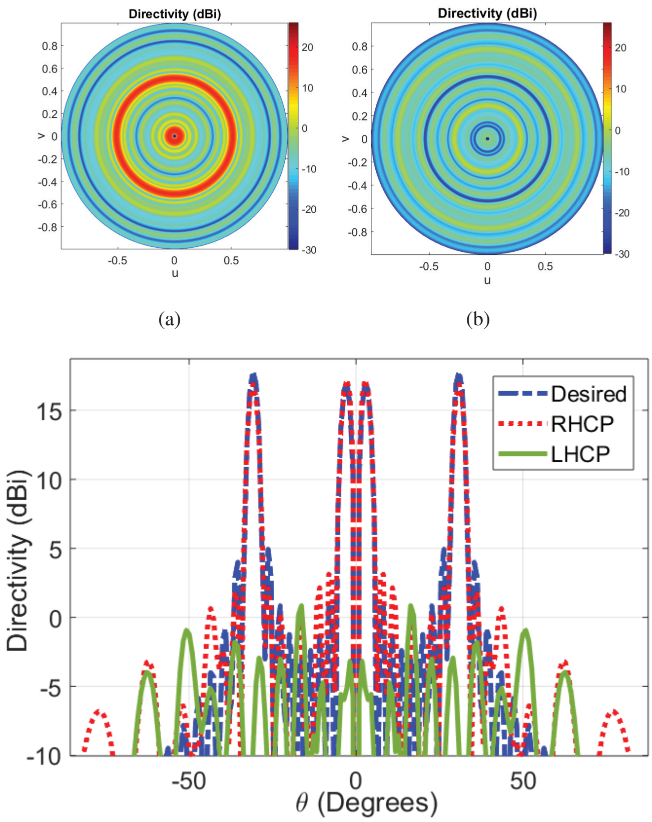

(c)

Fig. 5: Radiation pattern of the designed circularly polarized multi-OAM beams MTS (a) RHCP component in the (u, v) plane (b) LHCP component in the (u, v) plane (c) Directivity cut in the plane $\phi = 0^o$. $(u, v) = (\sin\theta\cos\phi, \sin\theta\sin\phi)$, where θ and ϕ respectively correspond to the elevation and azimuthal angles.

REFERENCES

[1] L. Allen, et al. , "Orbital angular momentum of light and the transformation of Laguerre-Gaussian laser modes", *Phys. Rev. A.,* vol. 45, no. 11, pp. 8185-8189, Jun. 1992.

[2] G. Gibson, et al. , "Free space information transfer using light beams carrying orbital angular momentum", *Opt. Exp.,* vol. 12, no. 22, pp. 5448-5456, 2004.

[3] M. Tamagone, C. Craeye, and J. Perruisseau-Carrier, "Comment on 'Encoding many channels on the same frequency through radio vorticity: First experimental test' ", *New J. Phys.,* vol. 14, pp. 118001, Nov. 2012.

[4] C. Craeye, "On the transmittance between OAM antennas", *IEEE Trans. Antennas Propag.,* vol. 64, no. 1, pp. 336-339, Jan. 2016.

[5] O. Edfors, and A. J. Johansson "Is orbital angular momentum (OAM) based radio communication an unexploited area", *IEEE Trans. Antennas Propag.,* vol. 60, no. 2, pp. 1126-1131, Feb. 2012.

[6] D. Mcgloin, and K. Dholakia "Bessel beams: diffraction in a new light", *Contemporary Physics.,* vol. 46, no. 1, pp. 15-28, Jan. 2005.

[7] M. Ettorre, et al. "Generation of propagating Bessel beams using leaky-wave modes", *IEEE Trans. Antennas Propag.,* vol. 60, no. 8, pp. 3605-3613, Aug. 2009.

[8] M. Albani, et al., "Generation of non-diffractive Bessel beams by inward cylindrical traveling wave aperture distributions", *Opt. Exp.,* vol. 22, no. 15, pp. 18354-18364, 2014.

[9] R. H. Caverly., "MRI Fundamentals: RF aspects of magnetic resonance imaging (MRI)", *IEEE Microwave Magazine.,* vol. 16, no. 6, pp. 20-33, Jul. 2015.

[10] C. L. Holloway, E. F. Kuester, J. Gordon, J. O'Hara, J. Booth and D. Smith "An overview of the theory and applications of metasurfaces: The twodimensional equivalents of metamaterials," *IEEE Antennas Propag. Mag.*, vol. 54, no. 2, pp. 10-35, 2012.

[11] N. Yu et al.,"Flat optics: Controlling wavefronts with optical antenna metasurfaces," *IEEE J. Sel. Topics Quantum Electron.,* vol. 19, no. 3, pp. 4700423, May. 2013.

[12] S. Maci, G. Minatti, M. Casaletti and M. Bosiljevac, "Metasurfing: Addressing waves on impenetrable metasurfaces," *IEEE Antennas Wireless Propag. Lett.*, vol. 10, pp. 1499-1502, Feb. 2011.

[13] G. Minatti, M. Faenzi, E. Martini, F. Caminita, P. De Vita, D. González-Ovejero, M. Sabbadini and S. Maci, "Modulated metasurface antennas for space: synthesis, analysis and realizations," *IEEE Trans. Antennas Propag.*, vol. 63, pp. 1288-1300, May. 2014.

[14] S. Mahmoud, Y. M. M. Antar, H. Hammad, and A. Freundorfer, "Theoretical considerations in the optimization of surface waves on a planar structure," *IEEE Trans. Antennas Propag.*, vol. 52, no. 8, pp. 2057-2063, Aug. 2004.

[15] M. Teniou, H. Roussel, N. Capet, G.-P. Piau, and M. Casaletti "Implementation of radiating aperture field distribution using tensorial metasurfaces," *IEEE Trans. Antennas Propag.*, vol. 65, pp. 5895-5907, Sep. 2017.

[16] A. Oliner, and A. Hessel,"Guided waves on sinusoidally-modulated reactance surfaces," *IRE Trans. Antennas Propag.*, vol. 7, no. 5, pp. 201-208, Dec. 1959.

[17] G. Minatti, F. Caminita, E. Martini, and S. Maci, "Flat optics for leaky-waves on modulated metasurfaces: adiabatic Floquet-wave analysis," *IEEE Trans. Antennas Propag.*, vol. 64, no. 9, pp. 3896-3906, Sep. 2016.

[18] M. Bodehou, C. Craeye, E. Martini, and I. Huynen, "A Quasi-direct method for the surface impedance design of modulated metasurface antennas," *IEEE Trans. Antennas Propag.*, vol. 67, no. 1, pp. 24-36, Jan. 2019.

[19] M. Bodehou, C. Craeye, and I. Huynen, "Electric field integral equation based synthesis of elliptical domain metasurface antennas," *IEEE Trans. Antennas Propag.*, vol. 67, no. 2, pp. 1270-1274, Feb. 2019.

[20] M. Bodehou, C. Craeye, H. Bui-Van, and I. Huynen, "Fourier-Bessel basis functions for the analysis of elliptical domain metasurface antennas," *IEEE Antennas Wireless Propag. Lett.*, vol. 17, pp. 675-678, April. 2018.

[21] D. González-Ovejero and S. Maci, "Gaussian ring basis functions for the analysis of modulated metasurface antennas," *IEEE Trans. Antennas Propag.*, vol. 63, pp. 3982-3993, Sep. 2015.

[22] M. Bodehou, D. González-Ovejero, C. Craeye and I. Huynen, "Method of Moments simulation of modulated metasurface antennas with a set of orthogonal entire-domain basis functions," *IEEE Trans. Antennas Propag.*, vol. 67, no. 2, pp. 1119-1130, Feb. 2019.

[23] M. Casaletti, M. Smierzchalski, M. Ettorre, R. Sauleau and N. Capet, "Polarized beams using scalar metasurfaces," *IEEE Trans. Antennas Propag.*, vol. 64, pp. 3391-3400, May. 2016.

[24] M. Bodehou, and C. Craeye, "Another field decomposition for the transmittance between OAM antennas," *FERMAT.*, vol. 24, no. 1, Nov. 2017.